RNA and will not quantitate DNA, protein, or free nucleotides. Moreover, it provides an assay range from 20 – 1000 ng, and the RNA starting concentration can be 1 ng/µl – 1 µg/µl.

Quantitation using this assay was performed at room temperature. The Working Solution was prepared in a sterile 2 ml Eppendorf tube containing BR reagent diluted 1:200 in BR buffer and briefly mixed by vortexing. The 2 Qubit® standards were prepared by adding 190 µl of working solution into 0.6 ml clear-walled, sterile tubes followed by 10 µl of the standard solutions. The standards were vortexed briefly and left to incubate at room temperature for two minutes.

The miRNA samples were prepared by diluting 2 µl of the sample with 198 µl of working solution (i.e. 1:100 dilution) in 0.6 ml clear-walled, sterile tubes. The sample was briefly vortexed and left to incubate at room temperature for two minutes.

Thereafter, the concentration of the standards were first read in order to calibrate the Qubit® 2.0 Fluorometer. Thereafter, the concentrations of the miRNA samples were determined. The Qubit® 2.0 Fluorometer has the option were it calculates the concentration using the following equation:

$$Concentration\ of\ unkwown\ sample = QF\ x\ \frac{200}{x}$$

Where QF = the value given by the Qubit® 2.0 Fluorometer, and *x* = volume (µl) of sample.

### 3.3.7. Primer synthesis

Mature miRNA sequences for each of the four miRNAs of interest and reference miRNAs were obtained from miRBase (http://www.mirbase.org/), as described in

section 2.2.1.1. Reference miRNAs used in this investigation shown to be stably expressed in kidney tissue was miR-17 and miRNA-191a (Eskildsen et al, 2013). Moreover, these reference miRNAs were found to be 100 % homologous to rats using the ClustalW sequence alignment tool (see description in section 2.2.1.1). GAPDH was used as a third reference gene, due to it displaying stable expression within kidney tissues as well (Ji et al, 2013).

The miRNA primers used for stem-loop RT-PCR was designed according to Kramer (2011). An example for miRNA primer design is given in Appendix B. Firstly, once the mature miRNA sequence of interest was obtained from miRBase, the RT stem-loop primer was designed. Designing the RT stem-loop primer combined the 44 nucleotide stem-loop sequence designed by Chen et al (2005) i.e. 5′- GTC GTA TCC AGT GCA GGG TCC GAG GTA TTC GCA CTG GAT ACG AC -3′ region to an additional six nucleotides, complimentary to the 3’ nucleotide from the mature miRNA sequence. Secondly, designing the forward primer involved taking the first 12 to 17 nucleotides of the 5’ end of the mature miRNA sequence and adding another three to seven random nucleotides to the 5’ end in order to increase the melting temperature (Tm) to aproximately 60 ˚C (± 1 ˚C) (Kramer, 2011). The OligoAnalyzer 3.1 tool (https://eu.idtdna.com/calc/analyzer) (Owczarzy et al, 2008) was used to calculate the estimated melting temperature for each forward primer. The reverse primer is universal since all RT stem-loop primers uses the same 44 nucleotide sequence. The sequence of the universal primer as recommended by Kramer (2011) is: 5′-CCA GTG CAG GGT CCG AGG TA-3′.

Reference genes used for normalization in kidney tissue was miR-191a, miR-17 (Eskildsen et al, 2013) and GAPDH (Ji et al, 2013). Primer sequences for reference miRNAs are given in Table 3.1. Primer sequences for GAPDH are as follows:

forward primer – TGATGACATCAAGAAGGTGGTGAAG; reverse primer: TCCTTGGAGGCCATGTGGGCCAT.

**Table 3.1:** Designed primer sequences for reference genes miR-191a and miR-17

| MiRNA name | Primer type | Sequence |
|---|---|---|
| rno-MiR-17-5p | Stem-loop RT primer | GTC GTA TCC AGT GCA GGG TCC GAG GTA TTC GCA CTG GAT ACG ACC TAC CT |
| | Forward primer | CCG TCA CCA AAG TGC TTA CAG TGC |
| | Reverse primer | CCA GTG CAG GGT CCG AGG TA |
| rno-MiR-191a-5p | Stem-loop RT primer | GTC GTA TCC AGT GCA GGG TCC GAG GTA TTC GCA CTG GAT ACG ACC AGC TG |
| | Forward primer | GAC GCT CAA CGG AAT CCC AAA AG |
| | Reverse primer | CCA GTG CAG GGT CCG AGG TA |

All primer oligonucleotide sequences were synthesised by Inqaba biotech (http://www.inqababiotec.co.za/). A 100 µM of stock solution of each primer was prepared in 1X TE buffer (10 mM Tris, pH 7.5 to 8.0, 1 mM EDTA). The concentrated stock oligonucleotide solutions and working stock solutions were stored at -20 ˚C.



### 3.3.8. cDNA synthesis

The Transcriptor First Strand cDNA Synthesis Kit protocol was slightly modified for cDNA synthesis from miRNA. A cocktail of miRNA-specific stem-loop (SL) primers was prepared (10 µM/primer, six primers in total). In sterile, nuclease-free PCR tubes, 3 µl template miRNA (~200 ng of miRNA), 2 µl SL cocktail primer, and PCR-grade water was added to make up a final volume of 13 µl. The primer mix was briefly centrifuged and then incubated in the GeneAmp® PCR System 2700 thermal block cycler at 65˚ C for five minutes, then placed on ice for two minutes, thereafter (Varkonyi-Gasic et al, 2007). After incubation, 4 µl Transcriptor Reverse Transcriptase Reaction Buffer (1X), 0.5 µl Protector RNase Inhibitor (20

U), 2 µl Deoxynucleotide mix (1 mM each), and 0.5 µl Transcriptor Reverse Transcriptase (10 U) was added to the primer mixture and gently mixed by finger tapping. The tubes were briefly centrifuged to bring all the contents down to the bottom of the tube and then placed in the thermal block cycler to perform pulse RT-PCR at the following parameters according to Varkonyi-Gasic (2007): 30˚ C for 30 seconds, 42˚ C for 30 seconds, and 50˚ C for one second for 60 cycles. The synthesised cDNA was stored at -20˚ C until needed for further analysis by conventional PCR and qRT-PCR.

### 3.3.9. Conventional PCR

The quality of miRNAs after extraction and cDNA synthesis was checked by performing conventional PCR, to observe if the primers do in fact bind to, and amplified, the cDNA template.

In sterile, nuclease-free PCR tubes, 12.5 µl KAPATaq EXtra HotStart ReadyMix and dye (1X), 1 µl of RT product (~ 100 ng), 1 µl forward primer (10 µM), 1 µl reverse primer (10 µM) was added and nuclease-free PCR-grade water to make up the reaction to a final volume of 25 µl. The reactions were placed on the thermal heating block and amplified according to the parameters shown in Table 3.2:

**Table 3.2:** Parameters used for conventional PCR reactions

| Step | Temperature (˚C) | Time | Cycle/s |
|---|---|---|---|
| Initial denaturation | 94 | 2 minutes | 1 |
| Denaturation | 94 | 15 seconds | 40 |
| Annealing* | 65 – 66.6 | 30 seconds | |
| Elongation | 60 | 1 minute | |
| Final elongation | 75 | 5 minutes | 1 |
| Cooling | 4 | ∞ | 1 |

*Annealing temperature is primer dependent

Thereafter, 10 µl of the amplified products was electrophoresed on 4 % agarose gel, stained with GelRed (stock 10, 000 X, diluted to 0.3 X when added to the molten agarose), at 90 V for 80 minutes, in 1X TBE running buffer (10X TBE stock: 1.2 M Tris, 1.2 M Boric acid, and 2 mM EDTA). Visualization was done with the BioSpectrum® Imaging System.



### 3.3.10. Quantitative real-time PCR

Real-time PCR (qRT-PCR) was performed using the SYBR Green miRNA assay according to the KAPA SYBR ® FAST qPCR kit protocol Optimized for LightCycler® 480. Reactions including the standards were carried out in 96-well, clear plates.

Each reaction was made up to a final volume of 10 µl with the following components: ~200 ng cDNA, 5 µl of 2X SYBR qPCR master mix, 1 µl of both forward and reverse primers at a concentration of 10 µM each, and nuclease-free, PCR-grade water. The LightCycler®480 was used to quantify differential expression according to the parameters shown in Table 3.3.

**Table 3.3:** Parameters used for qRT-PCR reactions

| Program | Step | Temperature (˚C) | Hold | Cycle | Fluorescence Acquisition |
|---|---|---|---|---|---|
| **Pre-incubation** | | 95 | 5 minutes | 1 | None |
| **PCR** | Denaturation | 95 | 10 seconds | 45 | None |
| | Annealing* | 64 | 20 seconds | | None |
| | Extension | 72 | 1 second | | Single |
| **Melting Curve** | Denaturation | 95 | 5 seconds | 1 | None |
| | Annealing | 65 | 1 minute | | None |
| | Extension | 97 | 5 – 10 acquisitions/˚C | | Continuous |
| Cooling | | | 30 seconds | 1 | None |

*Annealing temperature is primer dependent

Thereafter, data on expression levels of the reference genes were determined in the form of crossing points/cycle threshold ($Cp/C_t$). And the PCR efficiencies were calculated using the Relative Expression Software Tool (REST®) (Pfaffl, 2002). All Ct values were taken into consideration using the following equation:

$$E = 10^{[-\frac{1}{Slope}]}$$

Lastly, the expression levels of all four miRNAs were determined relative to the reference genes, using the following equation (Pfaffl, 2001):

$$R = \frac{(E\ target)^{\Delta Cp}.target^{(control\ sample)}}{(E\ ref)^{\Delta Cp}.ref^{(control\ sample)}}$$

## 3.4. Results

### 3.4.1. MiRNA extraction

Tissue from four HFD (T2DM), three T1DM, and three normal (control) were extracted from male Wistar rats as described in section 3.3.6. Due to the small size of miRNAs, agarose gel electrophoresis was not carried out. However, all isolated miRNA samples were quantified using the Qubit® Fluorometer 2.0 as described in section 3.3.6.1.

### 3.4.2. CDNA synthesis

The stem-loop reverse transcription method was used to synthesise cDNA for all the miRNA samples as described in section 3.3.8. The resulting cDNA samples were then quantified using the Thermo Scientific NanoDrop ND-1000 Spectrophotometer.



### 3.4.3. Conventional PCR

A conventional PCR was performed using cDNA from the four miRNAs of interest (mir-*dr*-1, miR-*ur*-1, miR-*ur*-2, and miR-*ur*-3) and the reference miRNAs: miR-191a and miR-17, as described in section 3.3.9. This was done to observe if the primers bound and aided in amplifying the targets of interest. It should be noted that a cDNA sample from a normal kidney tissue was used to test whether miRNAs of interest amplified.

From the results shown in Figure 3.2, expected bands of approximately 70 bp was observed for all miRNAs after agarose electrophoresis. Moreover, some bands were more intense than others, this could be due to these miRNAs having different expression levels within the control sample.

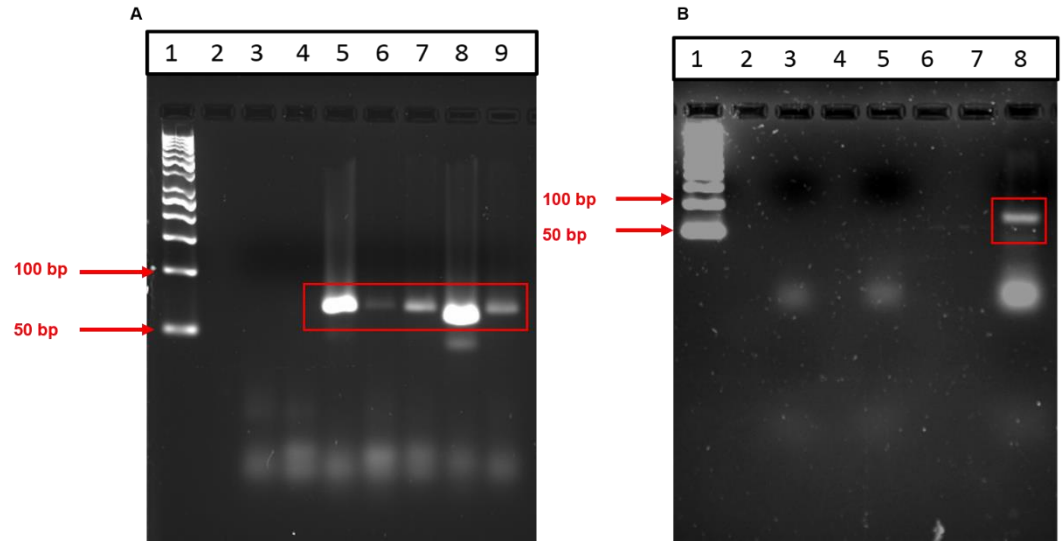


**Figure 3.2: PCR amplification of the control and test miRNAs.** A) LANE 1: 50 bp DNA ladder, LANE 2: empty, LANE 3 and LANE 4: control containing no template, LANE 5: normalisation miRNA mir-17, LANE 6: miR-*dr*-1, LANE 7: miR-*ur*-2, LANE 8: mir-*ur*-3, and LANE 9: normalization miRNA mir-191. B) LANE 1: 50 bp DNA ladder, LANE 3 and LANE 5: control containing no template, and LANE 8: miR-*ur*-1.



### 3.4.2. qRT-PCR analysis

#### *3.4.2.1. Standardisation of qRT-PCR*

The sets of crossing points for the reference genes were imported into REST® (Relative Expression Software Tool) in order to normalize the relative quantification of the microRNAs (miRNAs) to the reference genes. A randomization test was performed to determine the factor of regulation and level of significance of each miRNA expression across the different tissue tested. The amplification plot for the reference gene GAPDH is shown in Figure 3.3 A. GAPDH is a suitable housekeeping gene and has been found to be stable in the different tissues tested. Figure 3.3 B shows the amplification plot for the miR-*dr*-1. In both Figure 3.3 A and B, evenly spread out slopes were observed. During the

qRT-PCR assays performed amplification efficiencies between 3.35 and 3.4 were obtained for the respective miRNAs, indicating that optimized qRT-PCR reactions were performed. The amplification curves for the rest of the test and other control miRNAs are given in Appendix C.

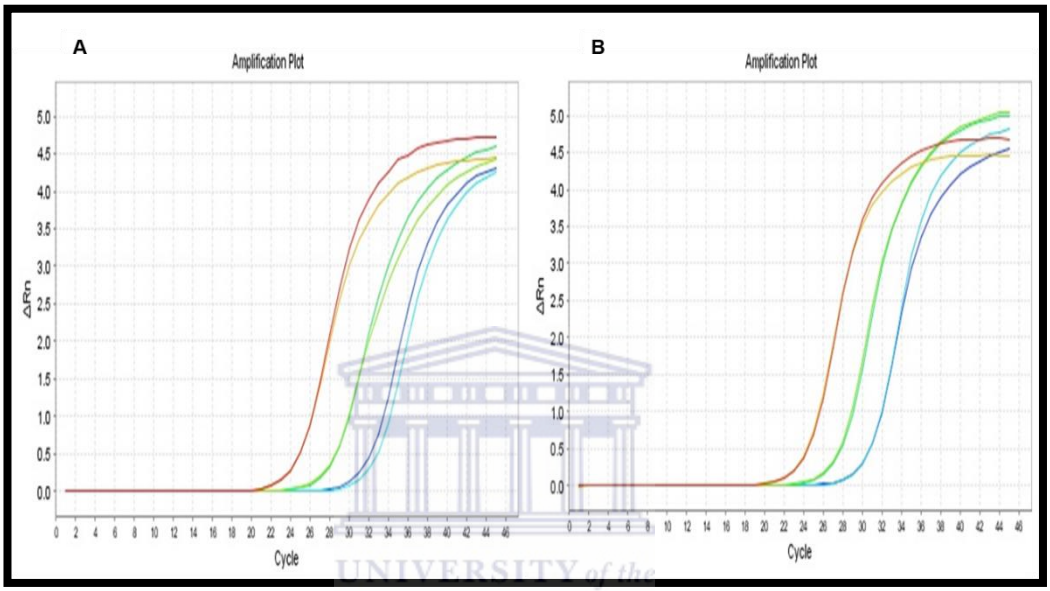




**Figure 3.3 (A)**: **Amplification plot for the reference gene, GAPDH, and miR-*dr*-1.** The red, green, and blue slopes indicate the amplification of GAPDH at the 1:10, 1:100, and 1:1000 dilutions, respectively. **(B)** The red, green, and blue slopes indicate the amplification of miR-*dr*-1 at the 1:10, 1:100, and 1:1000 dilutions, respectively.

### *3.4.2.2. Melting curve analysis*

A melting curve ranging from 60°C to 95°C was constructed for every reference and target gene/miRNA. The obtained melting curves were used to determine whether any contamination, mis-priming (referring to the annealing of primers to complementary sequences on non-target DNA), primer-dimers (primers annealing

to themselves), or other problems occurred. The melting curve for the reference gene GAPDH and miR-*dr*-1 are shown in Figure 3.4 A and B.

As the peaks in both figures are similar, it suggests that no contamination, mis-priming or primer-dimers are present. Only one peak is observed (one $T_m$) per gene, indicating that only one amplicon was amplified. Therefore, no non-specific amplification occurred and it is evident that accurate quantification of the genes of interest has been achieved through optimized qRT-PCR. The melting curve plots for the rest of the test and control miRNAs are given in Appendix C.

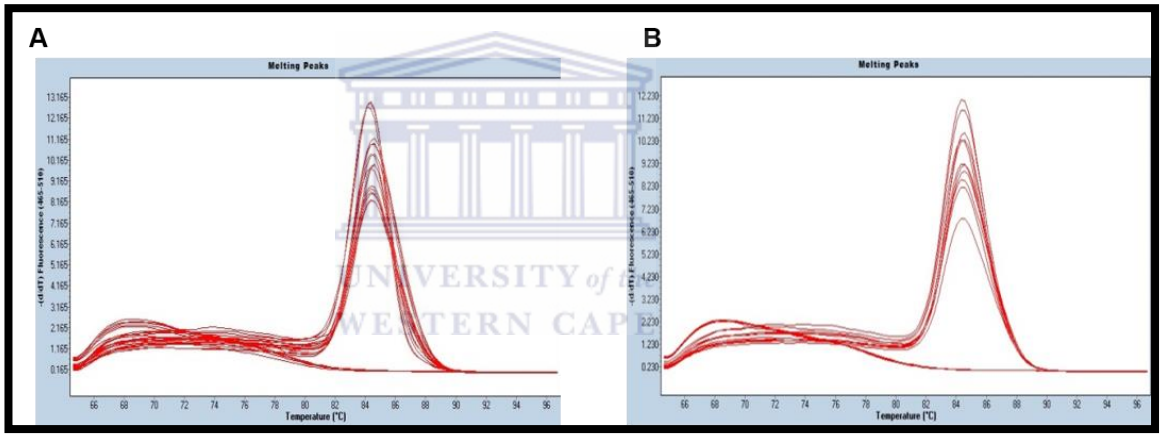


**Figure 3.4:** Melting curve analysis ranging from 65 ˚C to 95 ˚C for A) the reference gene, GAPDH, and B) miR-*dr*-1.

### *3.4.2.3. Reference genes: statistical analysis*

The accuracy of qRT-PCR is heavily dependent on the proper normalization of expression data, therefore, inappropriate normalization of qRT-PCR data can lead to incorrect conclusions (Peltier and Latham, 2008, Roberts et al, 2014). Thus, the main aim of reference genes is to remove variations between groups – the variations in this instance is caused by the disease (Peltier and Latham, 2008) or by experimental error. Ideally, a reference gene is a single nucleic acid that exhibits

constant expression across all samples, is expressed along with the target of interest within cells, and shows equivalent storage, stability, extraction, and quantification efficiency as the specific target of interest (Pfaffl, 2001; Peltier and Latham, 2008). However, a reference gene such as this does not exist in reality (Peltier and Latham, 2008).

MiRNAs, particularly, poses a significant challenge for normalization. This is thought to be due to miRNAs only representing 0.01 % of the mass amount of total RNA and this fraction can have significant variation across different samples (Peltier and Latham, 2008). Despite these challenges, however, there are three normalization strategies which aid in expression profiling of miRNAs which include (i) average of all the quantification cycles values (Cq) from the experiments, (ii) stably expressed endogenous reference miRNAs, and (iii) external spike-in synthetic oligonucleotides. In this investigation, miR-17 (Eskildsen et al, 2013), miR-191a (Eskildsen et al, 2013) and GADPH (Ji et al, 2013) were used as reference genes for normalization, based on previous studies which identified them to be stably expressed in kidney tissue. The expression of these reference genes were profiled in the different kidney tissue samples to test whether they had the same expression i.e. in the normal, HFD (T2DM), and T1DM kidney tissue samples. In this investigation, miR-17 was used for normalization due it exhibiting the same expression in all sample types (shown in Figure 3.5).

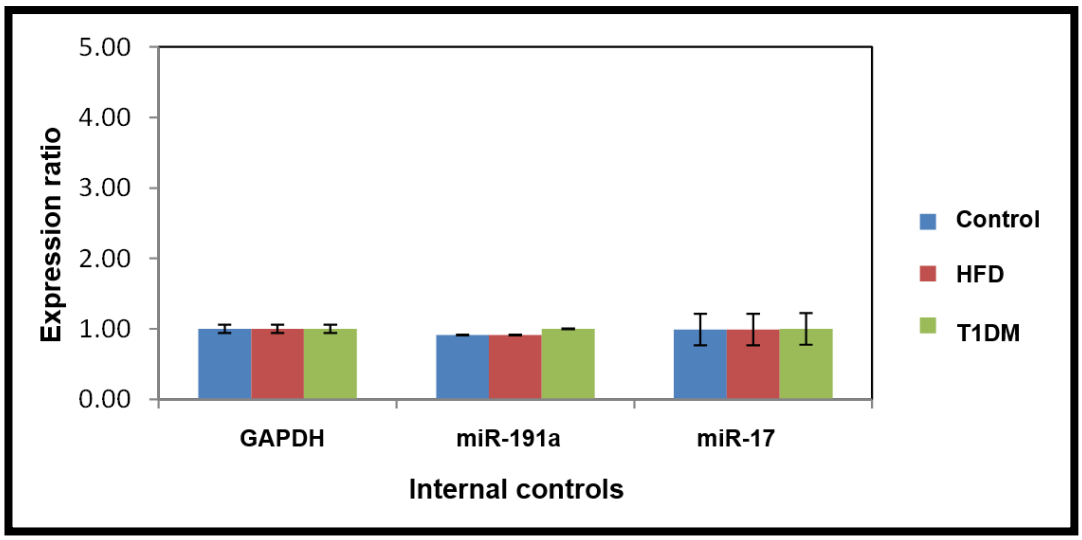


**Figure 3.5:** Expression levels of the reference genes in control tissue sample compared to HFD (T2DM) and T1DM samples



*3.4.2.4. Expression analysis of the 4 miRNAs of interest in HFD (T2DM) and TIDM tissues.*

For the expression analysis performed for the 4 miRNAs of interest in normal, T1DM, and HFD (T2DM) kidney tissue samples, ~ 200 ng of miRNA was extracted from the tissues, as described in section 3.3.6, and reverse transcribed to cDNA as described in section 3.3.8. A serial dilution ranging from 1:10 to 1:10 000 was performed using the cDNA obtained after reverse transcription. The cDNA was used in qRT-PCR reactions as described in section 3.3.10. The expression levels of the target miRNA were normalized against the expression of the reference gene (GADPH) and the two control miRNAs (miR-17). Furthermore, the expression ratios were determined using the REST® software package. The values obtained from the software package were exported to an Excel spreadsheet and a table was created containing all the descriptive statistics as indicated in Table 3.4.

From the results obtained for Table 3.4 it is shown that three of the miRNAs, miR-*ur*-1, miR-*dr*-1 and miR-*ur*-2, showed differential expression in the HFD (T2DM) samples when compared to the control samples. MiR-*ur*-1 was up-regulated in the HFD (T2DM) samples with a factor of 4.2 and a p-value of 0.05. MiR-*dr*-1 and miR-*ur*-2 were down-regulated in the HFD (T2DM) samples with a factor of 2.96 and 3.6 respectively, with p-values of 0.02 and 0.001. MiR-*ur*-3 was slightly up-regulated with a factor of 1.2 but this was not statistically significant, due to it having a p-value of 0.55.

In Figure 3.6, the expression ratios of all 4 miRNAs of interest are shown relative to the expression level in the control samples, where the control samples are given as an arbitrary value of one which indicates no variation of regulation of the four miRNAs.

**Table 3.4:** Relative expression ratio of the four miRNAs of interest in HFD (T2DM) kidney tissue samples compared to normal (control) kidney samples.

| Gene | Sample | Mean $C_T$ | Std. error | Fold change | p-value |
|---|---|---|---|---|---|
| ***miR*-ur-*1*** | Control | 34.93 | 0.07 | 4.2 | 0.05 |
| | HFD | 32.70 | 0.11 | | |
| ***miR*-dr-*1*** | Control | 34.90 | 0.10 | -2.96 | 0.02 |
| | HFD | 36.33 | 0.16 | | |
| ***miR*-ur-*2*** | Control | 34.17 | 0.15 | -3.6 | 0.001 |
| | HFD | 35.87 | 0.13 | | |
| ***miR*-ur-*3*** | Control | 32.20 | 0.13 | 1.2 | 0.55 |
| | HFD | 31.82 | 0.12 | | |
| ****HKG*** | Control | 28.19 | 0.04 | 1.098 | 0.209 |
| | HFD | 28.05 | 0.11 | | |

*HKG = Housekeeping gene

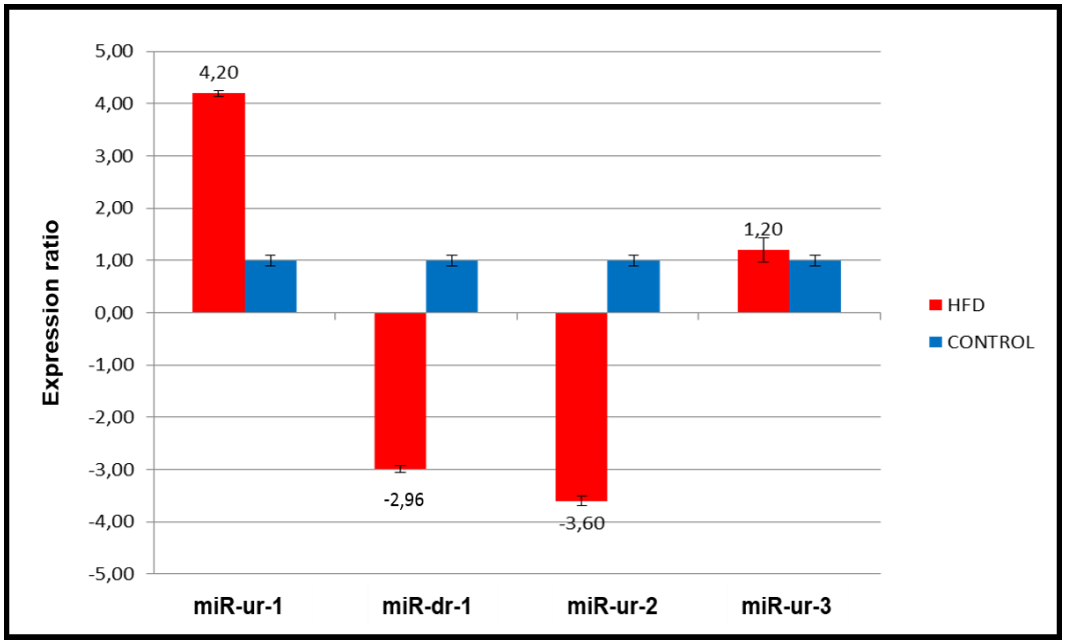


**Figure 3.6:** Relative expression ratio plot of the four miRNAs in normal kidney tissue compared to HFD (T2DM) kidney tissue.

Table 3.5 represents the descriptive statistics for the expression of the 4 miRNAs in T1DM samples. From the results obtained in Table 3.5 it is shown that all of the miRNAs showed differential expression in T1DM when compared to the control samples. Three miRNAs, i.e. miR-*ur*-1, mir-*dr*-1, and miR-*dr*-2, were found to be down-regulated in T1DM with a factor of 7.65, 3.25 and 2.77 respectively, with p-values of 0.001. However, miR-*ur*-3 was slightly up-regulated with a factor of 1.86 with a p-value of 0.05

In Figure 3.7, the expression ratios of all 4 miRNAs in T1DM are shown relative to the expression level in the control samples, where the control samples are a given an arbitrary value of one which indicates no variation of regulation of the miRNAs of interest.

**Table 3.5:** Relative expression ratio of the four miRNAs of interest in T1DM kidney tissue samples compared to normal (control) kidney samples.

| Gene | Sample | Mean $C_T$ | Std. error | Fold change | p-value |
|---|---|---|---|---|---|
| ***miR*-ur-*1*** | Control | 34.36 | 0.08 | | |
| | TID | 37.17 | 0.11 | -7.65 | 0.001 |
| ***miR*-dr-*1*** | Control | 32.53 | 0.21 | | |
| | TID | 34.10 | 0.10 | -3.25 | 0.001 |
| ***miR*-ur-*2*** | Control | 34.87 | 0.13 | | |
| | TID | 36.2 | 0.12 | -2.77 | 0.001 |
| ***miR*-ur-*3*** | Control | 32.13 | 0.07 | | |
| | TID | 31.06 | 0.15 | 1.864 | 0.05 |
| ****HKG*** | Control | 28.19 | 0.04 | | |
| | TID | 28.05 | 0.11 | 1.098 | 0.209 |

*HKG = Housekeeping gene

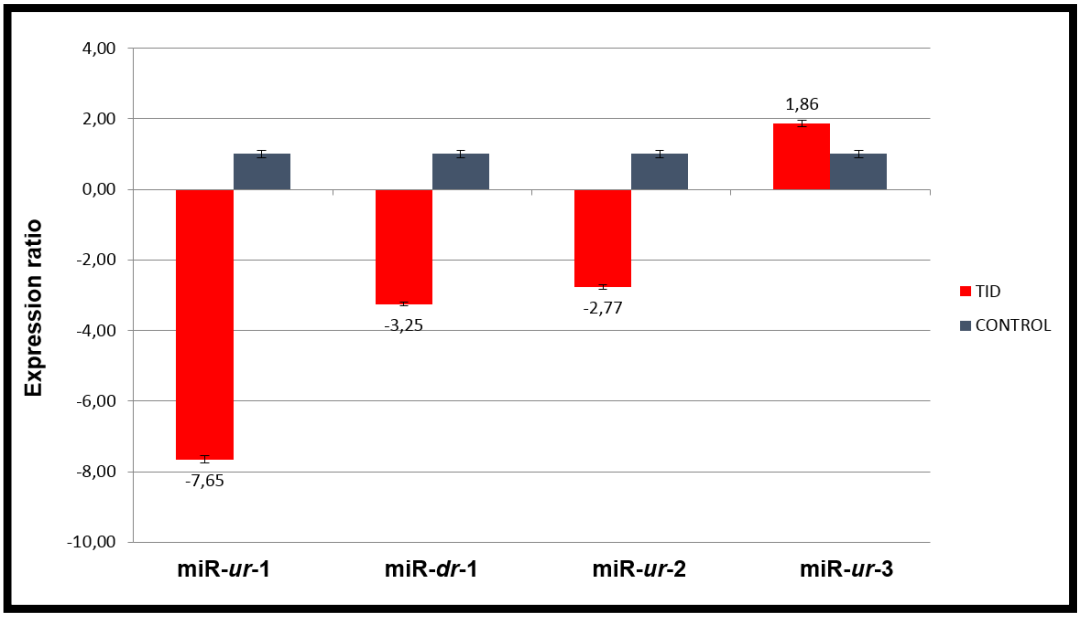


**Figure 3.7:** Relative expression ratio plot of the four miRNAs in normal kidney tissue compared to T1DM kidney tissue.



### *3.4.2.5. Summary*

Validation of biomarkers is an important step in biomarker discovery, as discussed in Chapter 1. Additionally, qRT-PCR is the golden standard for validation studies, and was, therefore, used in this investigation.

In this study, we evaluated the expression of four of miRNAs found to have differential expression in the serum/plasma of T2DM, as shown from the data obtained from various databases in section 2.2.1, and compared it to the expression in HFD (T2DM), T1DM and normal rat kidney tissues using qRT-PCR. The results indicate that three of these miRNA, i.e. miR-*ur*-1, miR-*dr*-1 and miR-*ur*-2, show significant differential expression in HFD (T2DM) rat kidney tissue, as shown in Table 3.2 and Figure 3.3. Whereas, all four miRNAs have significant differential expression in T1DM. The results obtained, therefore, indicates that these miRNA could potentially be used as predictive biomarkers in HFD (T2DM) and TIDM.

The miRNA which showed the most significant expression between T1DM and the HFD (T2DM) tissue samples, is miR-*ur*-1. This would be an ideal biomarker because it would clearly differentiate between T1DM and T2DM due to it being significantly up-regulated in HFD (T2DM) tissue samples, have a fold expression ratio of 4.2, and significantly down-regulated in T1DM tissue samples, as it had a fold expression ratio of -7.65 (see Table 3.6 below). The target genes that were predicted for miR-*ur*-1 in Chapter 2 were FOXP2, SIX5, and CACNB2.

Of these three genes, CACNB2 (calcium channel, voltage-dependent, beta 2) would be a target gene of interest. A study done by Lin et al (2011) found that variations of this gene is linked with hypertension. Furthermore, diabetic nephropathy (kidney failure) is the most common cause of hypertension (Lago et al, 2007). Furthermore, hypertension is also commonly linked with central obesity; which is one of the risk factors for T2DM (Lago et al, 2007).



**Table 3.6:** Summary of fold expression ratios of the 4 miRNAs of interest in HFD (T2DM) and T1DM rat kidney tissue samples

| Sample Type | miR-*dr*-1 | miR-*ur*-1 | miR-*ur*-2 | miR-*ur*-3 |
|---|---|---|---|---|
| **HFD** | **-2.96*** | **4.2*** | **-3.6*** | 1.2 |
| **T1DM** | **-3.25*** | **-7.65*** | **-2.77*** | 1.864 |

*Significant fold expression ratios are in red, bold font.

Furthermore, in the beginning of this chapter, a hypothesis was made that similar expression would be found in HFD (T2DM) rat kidney tissues as compared to

serum/plasma of T2DM, due to kidneys playing an important role in cleansing the blood from impurities.

Based on the results only three miRNAs i.e. miR-*dr*-1, miR-*ur*-1 and miR-*ur*-3 showed similar expression in rat kidneys as found in serum/plasma (which was obtained from the two databases as described in section 2.2.1) after qRT-PCR analysis (Table 3.5). However, miR-*ur*-2 was the only one which never showed similarity in expression compared to serum/plasma samples, and displayed significantly down-regulated expression in the HFD (T2DM) kidney tissue sample. A possible explanation for the contrasting expression in tissue and blood could be due to the alterations in the degradation of the miRNAs in circulation because more RNA degrading enzymes are present in circulation (Saikumar et al, 2012).

## 3.5. References


- Czimmerer, Z., Hulvely, J., Simandi, Z., Varallyay, E., Havelda, Z., Szabo, E., Varga, A., Deszo, B., Balogh, M., Horvath, A., Domokos, B., Torok, Z., Nagy, L. and Balint, B.L. 2013. A versatile method to design stem-loop primer-based quantitative PCR assays for detecting small regulatory RNA molecules. *PloS ONE*, 8(1): e55168
- Dedeoğlu, B.G. 2014. High-throughput approaches for microRNA expresson analysis. *Methods in Molecular Biology*, 1107(2014): 91 – 103
- Eskildsen, T., Jeppesen, P., Schneider, M., Nossent, A., Sandberg, M., Hansen, P., Jensen, C., Hansen, M., Marcussen, N., Rasmussen, L., Bie, P., Andersen, D. and Sheikh, S. 2013. Angiotensin II regulates microRNA-132/-212 in hypertensive rats and humans. *International Journal of Molecular Sciences*, 14(6): 11190 – 11207
- Huisamen, B., George, C., Dietrich, D. and Genade, S. 2013. Cardioprotective and anti-hypertensive effects of Prosopis glandulosa in rat models of pre-diabetes: cardiovascular topics. *Cardiovascular Journal of Africa*, 24(2): 10 – 16
- Ji, H., Wang, J., Liu, J., Guo, J., Wang, Z., Zhang, X., Guo, L. and Yang, H. 2013. Selection of Reliable Reference Genes for Real-time qRT-PCR Analysis of Zi Geese (*Anser anser domestica*) Gene Expression. *Asian-Australasian Journal of Animal Sciences*, 26(3): 423 – 432
- Kramer MF. 2011. Stem-loop RT-qPCR for miRNAs. *Current Protocols in Molecular Biology*, 15:1 – 5

- Lago, R.M., Singh, P.P. and Nesto, R.W. 2007. Diabetes and hypertension. *Nature Clinical Practice Endocrinology & Metabolism*, 3(10): 667
- Lin, Y., Lai, X., Chen, B., Xu, Y., Huang, B., Chen, Z., Zhu, S., Yao, J., Jiang, Q., Huang, H., Wen, J. and Chen, G. 2011. Genetic variations in CYP17A1, CACNB2 and PLEKHA7 are associated with blood pressure and/or hypertension in She ethnic minority of China. *Atherosclerosis*, 219(2): 709 – 714
- Owczarzy, R., Tataurov, A., Wu, Y., Manthey, J., McQuisten, K., Almabrazi, H., Pedersen, K., Lin, Y., Garretson, J., McEntaggart, N., Sailor, C., Dawson, R. and Peek, A. 2008. IDT SciTools: a suite for analysis and design of nucleic acid oligomers. *Nucleic Acids Research*, 36(Web Server): W163 – W169
- Peltier, H. and Latham, G. 2008. Normalization of microRNA expression levels in quantitative RT-PCR assays: Identification of suitable reference RNA targets in normal and cancerous human solid tissues. *RNA*, 14(5): 844 – 852
- Pfaffl, M. 2001. A new mathematical model for relative quantification in real-time RT-PCR. *Nucleic Acids Research*, 29(9): e45
- Pfaffl, M., Horgan, G.W. and Dempfle, L. 2002. Relative expression software tool (REST©) for group-wise comparison and statistical analysis of relative expression results in real-time PCR. *Nucleic Acids Research*, 30(9): e36.

- Saikumar, J., Hoffmann, D., Kim, T., Gonzalez, V., Zhang, Q., Goering, P., Brown, R., Bijol, V., Park, P., Waikar, S. and Vaidya, V. 2012. Expression, circulation, and excretion Profile of microRNA-21, -155, and -18a following acute kidney injury. *Toxicological Sciences*, 129(2): 256 – 267
- Stokowy, T., Eszlinger, M., Świerniak, M., Fujarewicz, K., Jarząb, B., Paschke, R. and Krohn, K. 2014. Analysis options for high-throughput sequencing in miRNA expression profiling. *BMC Research Notes*, 7(1): 144.
- Usó, M., Jantus-Lewintre, E., Sirera, R., Bremnes, R. and Camps, C. 2014. miRNA detection methods and clinical implications in lung cancer. *Future Oncology*, 10(14): 2279 – 2292
- van Rooij, E. 2011. The art of microRNA research. *Circulation Research*, 108: 219 – 234
- Varkonyi-Gasic, E., Wu, R., Wood, M., Walton, E.F., and Hellens, R.P. 2007. Protocol: a highly sensitive RT-PCR method for the detection and quantification of microRNAs. *Plant Methods*, 3: 12
- Wu, R., Wood, M., Thrush, A., Walton, E.F. and Varkonyi-Gasic, E. 2007. Real-time PCR quantification of plant miRNAs using universal ProbeLibrary technology. *Biochemica*, 2: 12 – 15

# Chapter 4: General discussion and Future work

Diabetes mellitus has made a significant impact on the non-communicable disease burden in South Africa (Volmink et al, 2014). Additionally, it has contributed considerably to mortality rates, causing 3.3 % of total deaths recorded in 2008 (Volmink et al, 2014). This mortality percentage has most likely increased since then.

The amount of individuals with T2DM, in particular, has increased rapidly over the years, as discussed in Chapter 1. However, unlike the other forms of diabetes, T2DM is the only type which can be prevented if diagnosed in its early stages i.e. pre-diabetes, by incorporating proper lifestyle habits, such as eating healthily and exercising regularly. Alternatively, it could also prevent the irreversible micro- and macrovascular complications linked with T2DM from developing. However, early diagnosis of T2DM rarely occurs and there are quite a number of individuals who are not even aware that they have the disease.



Despite current methods such as the OGTT and FPG tests being the most commonly used methods for screening diabetes in a clinical setting, there are limitations linked with them such as it being invasive as all tests require a blood sample, patients are required to fast beforehand, some tests are time-consuming for both the patient and health professional, and tests like the HbA1c tests are expensive. Lastly, these tests can not differentiate between the types of diabetes

the individual may have. There is, therefore, a need for biomarkers which can detect pre-diabetes and T2DM without having the aforementioned limitations.

MiRNAs has shown promise as ideal biomarkers for diagnostic, prognostic and therapeutic purposes for many diseases, as well as T2DM. Thus, the main purpose of this study was to identify potential miRNAs as new biomarkers for the early detection of T2DM. This study was split into two methodologies i.e. *in silico* and molecular identification.

The objectives for the *in silico* study involved identifying miRNAs found to be differentially expressed in the serum/plasma of T2DM individuals, identifying their target genes and their mechanism of action using several web-based *in silico* tools. This study successfully identified four miRNAs (miR-*dr*-1, miR-*ur*-1, miR-*ur*-2, and miR-*ur*-3) as well as their target genes, and thus may be used as biomarkers for the early detection of T2DM. All the miRNAs of interest play a role in the insulin signalling pathway. Furthermore, due to the fact that the *in silico* methodology by Masotti and Alisi (2013) identified known genes linked with T2DM (LDLR, PPARA, CAMTA1, IGF2BP2, and ANK2) suggests that using this methodology, can be considered credible. However, one should bear in mind that *in silico* prediction of biomarkers should be validated using appropriate *in vitro* laboratory techniques (Ngcoza, 2013).



In this study, miR-*dr*-1 and its two target genes, LDLR and PPARA, was found to be of particular interest, seeing as STRING analysis found an interaction between the two genes. Additionally, as described in section 2.4.2.2, the study conducted by Bernal-Mizrachi et al (2003) found that LDLR deficient mice, with

PPARA (+/+), eventually developed insulin resistance when continuously treated with glucocorticoids. Therefore, it would be worth validating miR-*dr*-1 to these target genes.

Furthermore, miR-*dr*-1 was predicted to target APP (amyloid precursor protein); a protein playing a main role in the pathology of Alzheimer's disease (AD) (Zhao and Townsend, 2009). Evidence showing a link between AD and T2DM has grown (Janson et al, 2004; Dandona et al, 2011). Recent studies have shown that glucose metabolism is severely impaired in the cerebral cortex of AD patients. More specifically, disruptions of the APP gene was shown to affect glucose metabolism and tolerance (Zhao and Townsend, 2009). Therefore, despite it not being discussed in Chapter 2, APP could be another target gene of interest that could be validated in future studies.



It should be noted that the identification of putative biomarkers using high-throughput *in silico* methods instead of traditional laboratory techniques could lead to the identification of a large number of novel biomarkers in a shorter period of time. Therefore, a molecular approach was employed to compare the differential expression of the 4 miRNAs found to be differentially expressed in serum/plasma of T2DM individuals (obtained from the databases in Chapter 2) to analyse expression levels in kidney tissue from HFD (T2DM), T1DM and normal male Wistar rats. The hypothesis was made that similar miRNA expression was expected for the HFD (T2DM) kidney tissue samples compared to serum miRNA expression levels found in T2DM (as shown in the databases),

due to the fact that kidneys play an important role in purifying the blood from impurities.

All expression profiles for the miRNAs were similar to expression in serum/plasma of T2DM, except for miR-*ur*-2. As discussed in the summary of Chapter 3, the possible reason for this inconsistency could be due to the alterations in degradation of miRNAs in circulation because there is a higher level of RNA degrading enzymes in circulation (Saikumar et al, 2012).

Based on the molecular analysis, miR-*dr*-1 had significant differential expression, thus, suggesting that this miRNA should be validated in future as a potential biomarker for T2DM. Interestingly, miR-*ur*-1 showed vast differences in expression between T1DM and T2DM samples, see section 3.4.2.4; it was significantly up-regulated in the HFD (T2DM) samples and significantly down-regulated in T1DM samples. Thus, this miRNA could possibly differentiate between the two types of diabetes. Due to the results obtained, it should be validated in the future.



## 4.1. Future work

Future work would include testing expression levels of the miRNAs of interest in T2DM induced rats, using the same methodology as described in sections 3.3.5 to 3.3.10. One of the shortcomings of this thesis was that there was not a large enough sample population. Therefore, more rat kidney samples i.e. normal, HFD, T1DM and T2DM, will be included for future studies. Once a miRNA which can

specifically and consistently discriminate between the normal, T1DM and T2DM rat kidney samples, comparison studies would be done in human blood and urine samples to determine if similar expression levels will be obtained as compared to the results achieved from this study.

Furthermore, urine and blood samples would be used in place of kidney samples when doing human studies as it would be invasive.

Furthermore, binding studies will be done for miR-*dr*-1 and its predicted target genes i.e. LDLR and PPARA, and miR-*ur*-1 and its predicted target gene CACNB2. A common method used for binding studies is the luciferase reporter gene assay; which is used to test the effect of miRNA-mediated, post-transcriptional regulation on the target genes (Jin et al, 2013). This is made possible by engineering a luciferase gene construct which contains the predicted miRNA target gene (Jin et al, 2013).



Lastly, if the target gene is predicted to be the true target of the miRNA of interest, an experiment will be done to test the effect of the miRNA on the specific target gene (Kuhn et al, 2008). A typical approach for this would be to transiently over-express the miRNA/s of interest (miRNA mimics would be used) within a cell type which is known to express the predicted target protein. The effect of the miRNA/s on the target gene would then be analysed either by Western blotting or ELISA (Kuhn et al, 2008). It is expected that if the miRNA of interest is overexpressed, the target gene will decrease in expression (Kuhn et al, 2008).

This study may greatly contribute to current research to identify biomarkers for alternative, non-invasive diagnostic methods for T2DM.

## References


- Bernal-Mizrachi, C., Weng, S., Feng, C., Finck, B., Knutsen, R., Leone, T., Coleman, T., Mecham, R., Kelly, D. and Semenkovich, C. 2003. Dexamethasone induction of hypertension and diabetes is PPAR-α dependent in LDL receptor–null mice. *Nature Medicine*, 9(8): 1069 – 1075
- Dandona, P., Mohamed, I., Ghanim, H., Sia, C., Dhindsa, S., Dandona, S., Makdissi, A. and Chaudhuri, A. 2011. Insulin suppresses the expression of amyloid precursor protein, presenilins, and glycogen synthase kinase-3β in peripheral blood mononuclear cells. *The Journal of Clinical Endocrinology & Metabolism*, 96(6): 1783 – 1788
- Janson, J., Laedtke, T., Parisi, J., O'Brien, P., Petersen, R. and Butler, P. 2004. Increased risk of type 2 diabetes in Alzheimer disease. *Diabetes*, 53(2): 474 – 481
- Jin, Y., Chen, Z., Liu, X. and Zhou, X. 2013. Evaluating the microRNA targeting sites by luciferase reporter gene assay. *Methods in Molecular Biology*, 936: 117 – 127
- Kuhn, D., Martin, M., Feldman, D., Terry, A., Nuovo, G. and Elton, T. 2008. Experimental validation of miRNA targets. *Methods*, 44(1): 47 – 54
- Ngcoza, N. 2013. *Identification of biomarkers in breast cancer as potential diagnostic and therapeutic agents using a combined in-silico and molecular approach*. MSc Thesis, University of the Western Cape

- Saikumar, J., Hoffmann, D., Kim, T., Gonzalez, V., Zhang, Q., Goering, P., Brown, R., Bijol, V., Park, P., Waikar, S. and Vaidya, V. 2012. Expression, circulation, and excretion Profile of microRNA-21, -155, and -18a following acute kidney injury. *Toxicological Sciences*, 129(2): 256 – 267
- Volmink, H.C., Bertram, M.Y., Jina, R., Wade, A.N. and Hofman, K.J. 2014. Applying a private sector capitation model to the management of type 2 diabetes in the South African public sector: a cost-effectiveness analysis. *BMC Health Services Research*, 14: 444
- Zhao, W. and Townsend, M. 2009. Insulin resistance and amyloidogenesis as common molecular foundation for type 2 diabetes and Alzheimer's disease. *Biochimica et Biophysica Acta (BBA) - Molecular Basis of Disease*, 1792(5): 482 – 496

# Chapter 5: Appendix - List of susceptibility genes from T2DGAD

| | | | | | | | | |
|---|---|---|---|---|---|---|---|---|
| TCF7L2 | GCK | CASQ1 | GCGR | KLF16 | FAM129A | UTS2R | SHBG | NKX6-1 |
| PPARG | APOE | PDE3B | NAMPT | MCF2L2 | GSTT1 | 10q21.1 | SULF2 | PHLDB1 |
| KCNJ11 | KCNQ1 | PTEN | VEGFA | NR1H3 | GSTM1 | 1p31.1 | WAC | PTPN22 |
| IGF2BP2 | HNF1B | STX1A | CDKN2A | PLAGL1 | IL1RN | 5p14.3 | 11p15.1 | SLC15A4 |
| HHEX | SOD2 | FOXO1 | HHEX | RBM18 | KLF6 | ADCY10 | 20p12.1 | TGIF2 |
| CDKAL1 | IAPP | HIF1A | IDE | SLC5A7 | MMP12 | ARHGEF12 | 5q35.3 | XRCC1 |
| SLC30A8 | JAZF1 | ANXA1 | INSR | 12q24.22 | NUCB2 | DDIT3 | AVPR1A | 11q22.3 |
| FTO | ADAMTS9 | CCL2 | PPARGC1B | 2q32.2 | SLC9A9 | FHIT | DLGAP4 | 6q14.1 |
| HNF4A | PPP1R3A | MC3R | RPL21P7 | 8p12 | TRPS1 | IMMT | HMBOX1 | C11ORF41 |
| ADIPOQ | PON1 | AHSG | SORBS1 | AKT1 | 14q12 | KRT4 | MTHFSD | EGR2 |
| CAPN10 | GNB3 | PLIN | APOC3 | CSE1L | 3p26.1 | MT1B | PAX4 | GC |
| ENPP1 | BTC | 13q21.1 | GSTT1 | ESRRG | 9q34.13 | OPRM1 | PPP3CA | MYL9 |
| CDKN2A | APOA5 | CSN3 | POMC | ICAM1 | CX3CR1 | RNLS | SAMD12 | PCK2 |
| CDKN2B | RBP4 | PYY | NPY | KL | EYA2 | UBR1 | SPDEF | SF1 |
| ACE | TSPAN18 | AGT | CAMTA1 | LTA | IFT52 | 16q21 | 18q12.1 | STAT4 |
| PPARGC1A | LGR5 | LDLR | 11q14.2 | PIGT | KLF12 | 4p14 | 4q24 | 10q21.3 |
| RETN | THADA | KLF7 | 20p13 | PTPRT | NQO1 | CD47 | ACTN2 | 1p34.3 |
| HNF1A | 11p12 | MMP26 | 6p25.2 | SLC25A27 | PKLR | CYP27B1 | APOM | 5q21.3 |
| EXT2 | SLC2A10 | A2BP1 | ADRA2B | THBS2 | RALGPS2 | FABP3 | CDK11A | ADCY3 |
| MTHFR | LEPR | MC4R | BCL11A | 11q23.2 | ANGPTL1 | GSTK1 | DBC1 | ARNT |
| TNF | MTTP | CRP | CHI3L1 | 20q13.12 | 12q21.2 | KLF2 | FAM60A | CDKN1C |
| LOC387761 | PBX1 | ESR1 | G6PC2 | 7p12.3 | 2q14.3 | MGEA5 | GYPC | DIO2 |
| ABCC8 | UCP3 | GFPT1 | ISL1 | AGER | 7q31.1 | NR3C1 | IL4 | FOXA2 |
| WFS1 | CDC123 | KCTD12 | PRKAB2 | C20orf24 | CPNE4 | RBM19 | NUDT12 | L3MBTL |
| ADIPOR2 | CAMK1D | 20q12 | SDF2L1 | CNTN1 | EPHX2 | SLC6A2 | PON2 | MT1E |
| IL6 | SLC2A2 | CLPS | SPRY1 | HPSE2 | GFM1 | TRPA1 | RICH2 | OR13D1 |
| UCP2 | ABCA1 | LIPC | ANKRD50 | KCNJ10 | HTR4 | 2q36.1 | SMAD7 | RORA |
| PDX1 | IL10 | PRKCZ | 10q11.21 | LMX1A | ADRB2 | 8q11.23 | TSC22D1 | SOD3 |
| NOS3 | IDE | VDR | 1p21.1 | NAP5 | LRGUK | ANGPT4 | 14q21.1 | 17p12 |
| PCK1 | NOTCH2 | UCP1 | 5p14.1 | SGK2 | NKX2-2 | CAT | 3q13.13 | 4p15.33 |
| HFE | C4orf32 | GSTM1 | CDK5 | VWF | PECAM1 | EXOC4 | AP2M1 | APOB |
| IRS1 | GCKR | NRF1 | DCD | 11p14.3 | SLC13A1 | GHSR | CCR5 | CD96 |
| INS | USF1 | 13q21.33 | HADH | 1q43 | WRN | KLF1 | CXCL5 | CYP3A4 |
| ADRB3 | PKN2 | AGTR1 | KLF9 | 5q34 | 11q21 | MAPK8 | F3 | FABP4 |
| UTS2 | ADRB2 | CACNA1E | MT1A | ATP5O | 20q11.23 | PIK3C2G | GPC5 | IL1B |
| GHRL | RAGE | BCHE | RNF34 | DLGAP2 | 6q13 | SLC27A5 | IGF1 | KLF3 |
| PTPN1 | MTNR1B | CETP | SOD1 | INSRR | ADRB1 | TLR4 | KLF13 | MIF |
| SREBF1 | LMNA | LEP | UBQLNL/OR52H1 | NTRK1 | CHRM3 | 11q24.1 | NR0B2 | PNPLA2 |

| | | | | | | | | |
|---|---|---|---|---|---|---|---|---|
| ADIPOR1 | KLF11 | PRKAA2 | 15q24.1 | LCORL | DYRK2 | 20q13.13 | RAPGEF1 | SLC8A1 |
| CDKN2B | LPL | SPINK1 | 3q26.31 | NCAPG | IFNG | 7p13 | TNFRSF4 | TRPM6 |
| NEUROD1 | DUSP12 | DBI | AACS | PARL | GAL3ST1 | COL13A1 | 12q21.31 | 3p12.3 |
| IRS2 | ARHGEF11 | 3q26.1 | APOA2 | RUNX2 | ITGB3 | ENSA | 2q21.2 | 8q21.3 |
| PPARA | FFAR1 | CD14 | CD36 | SOS1 | LINGO2 | HSD11B1 | 7q31.33 | ANK2 |
| NEUROG3 | OGG1 | CXCR4 | CYP11B2 | 18p11.31 | MYBL2 | NDRG3 | AKAP10 | CCDC138 |
| IL6R | PPARD | AKR1B1 | GRIK1 | 4q13.3 | PRKCB | PDE4B | CARTPT | CTLA4 |

| | | |
|---|---|---|
| IDE | APOA1 | PANK4 |
| HHEX | F7 | 17q24.3 |
| KIF11 | GRB10 | 4q13.1 |
| KLF10 | KLF14 | ABCC9 |
| MC2R | MC5R | CDC123 |
| NPPB | NR1H2 | CYP3A5 |
| PIK3CB | PLA2G4A | FABP6 |
| SLC2A1 | RASGEF1A | IL1RAP |
| TMCO7 | SLC44A3 | KLF5 |
| 12q13.11 | TOP1 | MMP1 |
| 21q21.3 | 12q22 | NRP1 |
| 7p21.3 | 2q22.1 | REG1A |
| COX7A1 | 7q32.3 | SLC9A8 |
| EPB41L3 | CASP9 | TRPM7 |
| GDAP1L1 | CRTC2 | 13q31.1 |
| HSPA1B | ESRRA | 3p24.3 |
| KCNJ9 | GFPT2 | 8q23.3 |
| LPIN2 | ICA1 | ANKRD50 |
| PDK4 | NXPH1 | CCDC60 |
| PTGIS | KIAA0319L | CWC22 |
| SIDT1 | LRP6 | EXT2 |
| TAS2R16 | PHLPP | ALX4 |
| 11p15.4 | PTPRS | GLP1R |
| 20p12.3 | SLC24A3 | IFNG |
| 6p12.3 | ZPBP | MC2R |
| DNAJC19 | 11q23.1 | MC5R |
| FXN | 20q13.11 | PIK3R1 |
| HMOX1 | 6q24.1 | RALGPS2 |
| PAX6 | C12orf75 | TMEFF2 |
| SCD | CLVS1 | 12q15 |
| UTRN | CHD7 | 2p13.2 |
| 18q21.2 | EIF2AK4 | 7q21.11 |
| 4q28.3 | HNRPUL1 | AHI1 |

| | | |
|---|---|---|
| ADAM30 | KCND2 | CPLX2 |
| NOTCH2 | PCLO | EPHB3 |
| ARFGEF2 | PRKG2 | GDNF |
| CDK4 | SGK1 | EGFLAM |
| FBXL17 | STK11 | HTR2C |
| GYS1 | 1q24.2 | KCNMB1 |
| KLF8 | 5q23.2 | PTGS2 |
| MSH6 | ADCYAP1 | SLA2 |
| ODZ2 | ATF6 | TCEB1 |
| RIMS1 | DKFZp686O24166 | WNT5B |
| SMC3 | FOXC2 | A2M |
| 14q31.1 | LARS2 | MT2A |

# Appendix B: Primer design example (adopted from Kramer, 2011)

**1. Quantification Standard**—This is the precise sequence of the miRNA of interest. Here, miR-H1, expressed by HSV-1 (Cui, 2006; Umbach, 2008; Jurak, 2010), will be used as an example.

The 20 nt RNA sequence of miR-H1 is the Quantification Standard:

5′-UGG AAG GAC GGG AAG UGG AA-3′

**2. Stem-Loop (SL) RT primer**—This combines 44 nt of the stem-loop sequence of Chen et al., 2005, 5′- GTC GTA TCC AGT GCA GGG TCC GAG GTA TTC GCA CTG GAT ACG AC -3′ with the complement of the six 3′ nt of the mature miRNA sequence (boxed)*This is the stem-loop RT primer for miR-H1:*

*5′- GTC GTA TCC AGT GCA GGG TCC GAG GTA TTC GCA CTG GAT ACG AC*

*TTC CAC* -3′

**3. Forward qPCR primer**—Together the Forward qPCR Primer and the Probe should maximally cover the mature miRNA sequence. Take the first 12 to 17 nt of the 5′ end of the mature miRNA, and 3 to 7 additional 5′ nt selected for getting the Tm to 60°C. Start with the first 12 nt, as in this example below, so as to maximize probe coverage of the remaining miRNA sequence.

a. Take the first twelve 5′ nt from the mature miRNA sequence (transformed to DNA, boxed)

5′- TGG AAG GAC GGG -3′

b. Add six nt to the 5′ end. The sequence of the six nt should be selected to confer upon the final oligo a Tm of 60 +/- 1 °C. An online calculator such as http:www.idtdna.com/analyzer/Applications/OligoAnalyzer can be useful. This is the miR-H1 Forward primer:

5′- CAC GCA TGG AAG GAC GGG -3′

**4. Reverse qPCR Primer**—By using the same 44 nt stem-loop sequence for all RT primers, a universal primer can be derived from sequences within the stem-loop. We recommend this Reverse Primer:

5′-CCA GTG CAG GGT CCG AGG TA-3′

*The reverse primer sequence reported by* Chen et al., 2005, *is: 5′- GTG CAG GGT CCG AGG T -3′. We found improved sensitivity with the longer primer.*

# Appendix C: Melting and amplification plots for all miRNAs

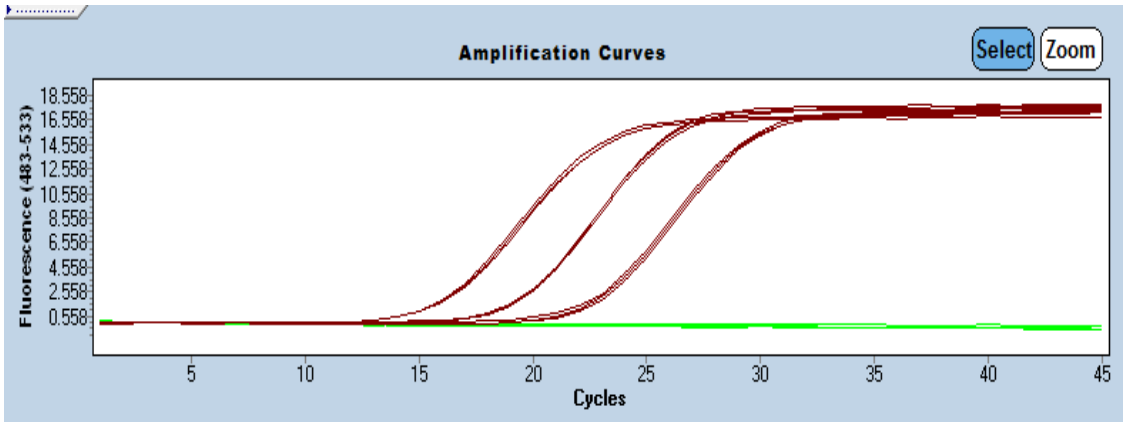


**MiRNA 17A – Amplification curve**



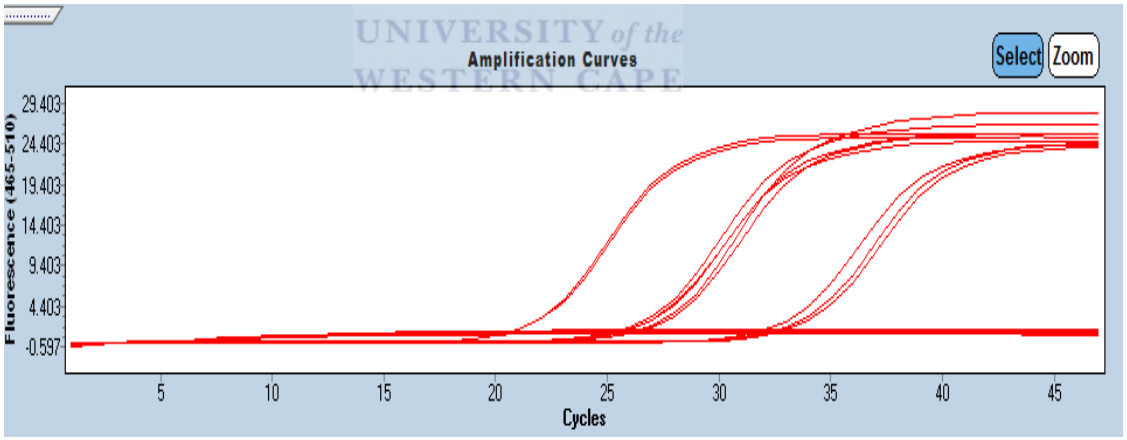


**MiRNA 191A – Amplification curve**

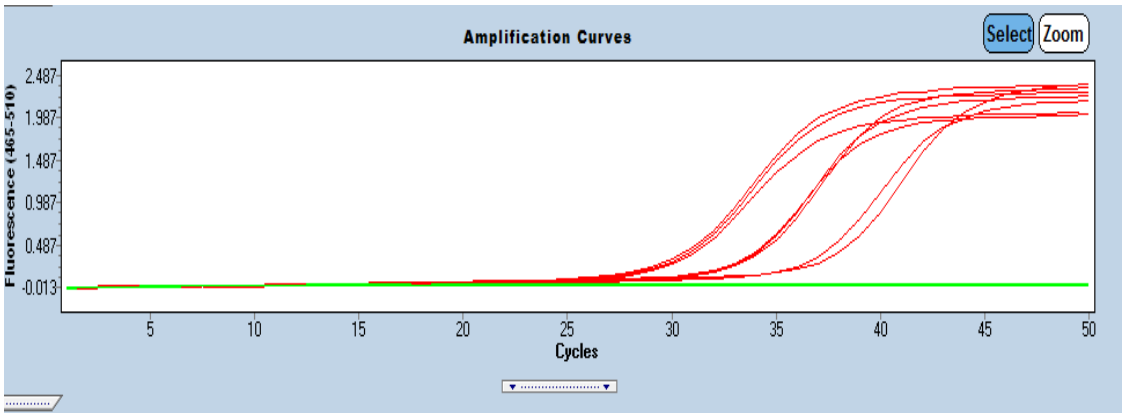


**Mir-ur-1 Amplification curve**



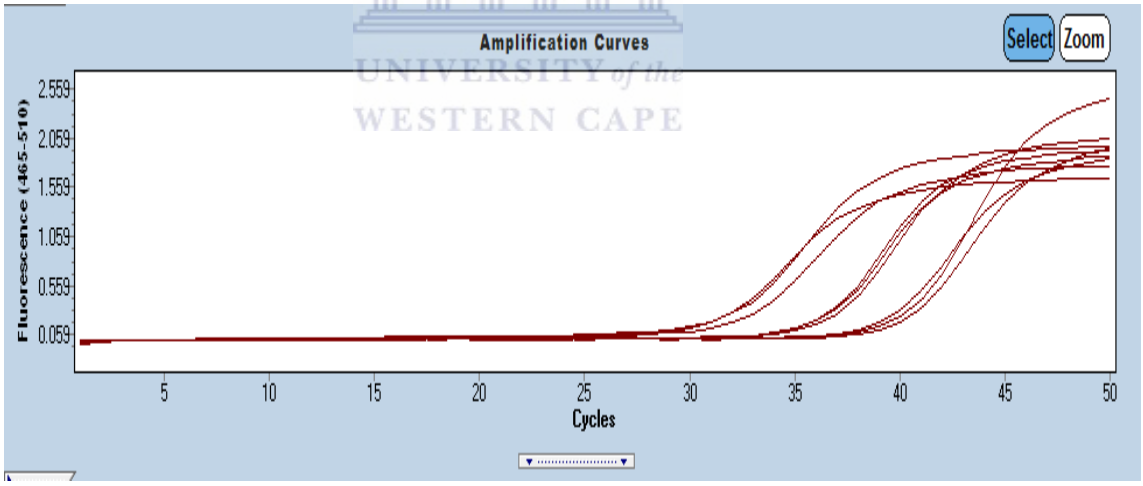


**Mir-ur-2 amplification curve**

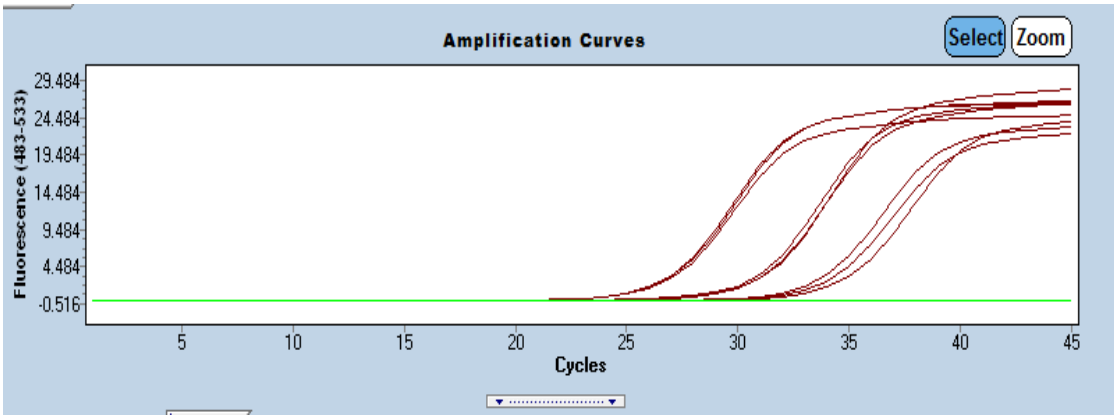


**Mir-ur-3 amplification curve**

## Melting Curves:

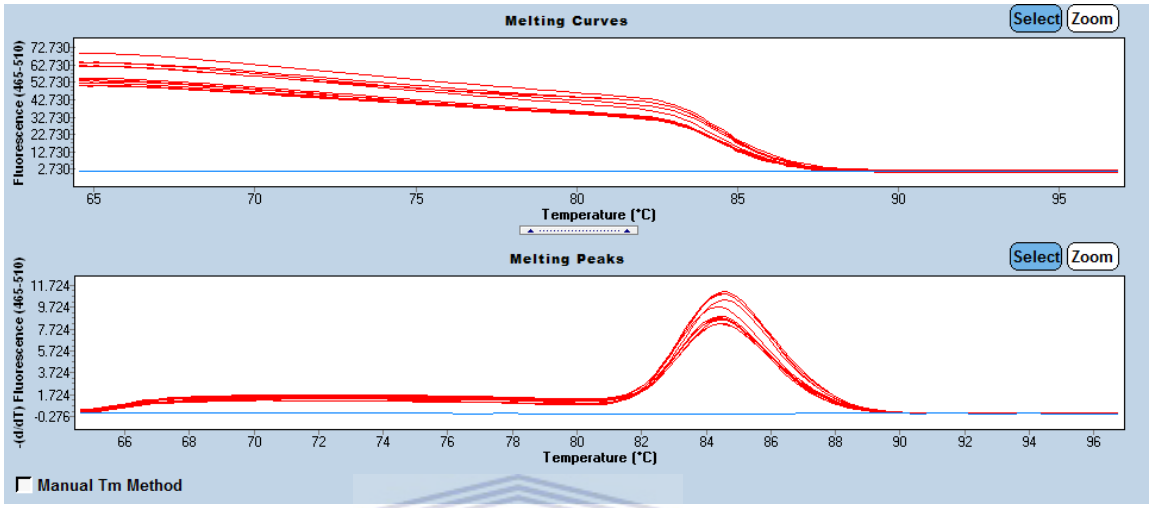


**MiRNA17A – melting curve**



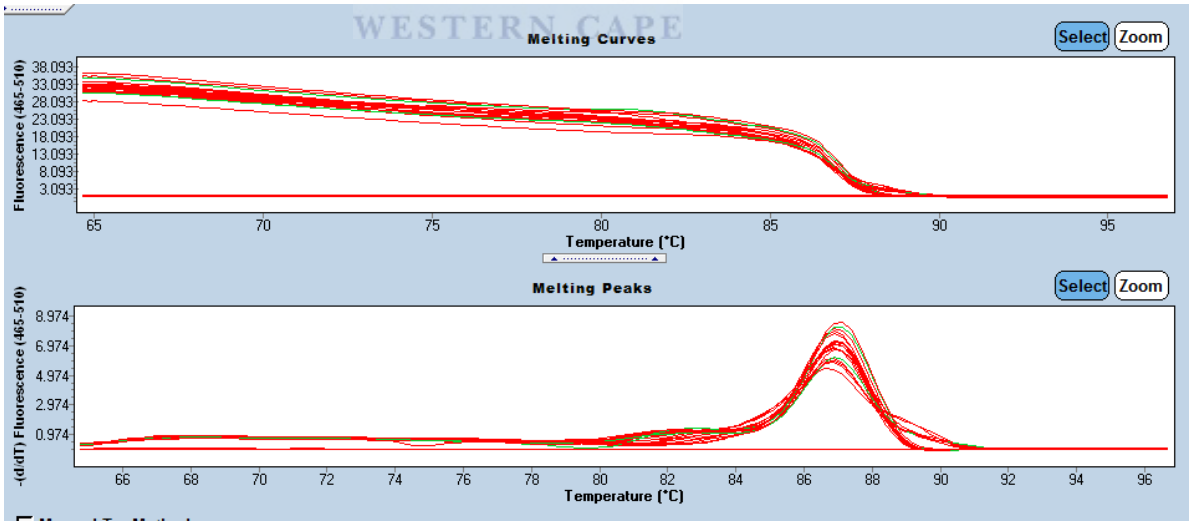


**MiRNA 191A- melting curve**

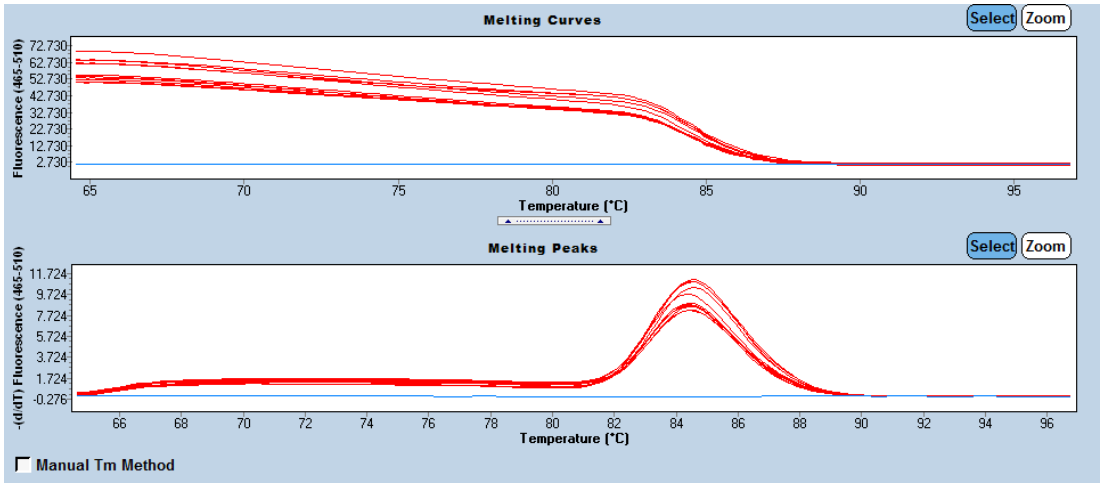


**Mir-ur-1 melting curve**

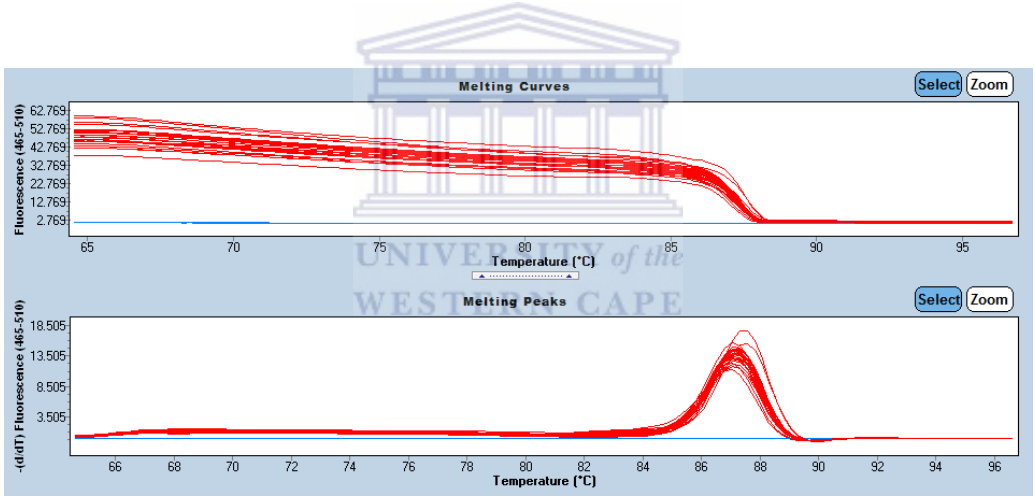




**Mir-ur-2 melting curve**

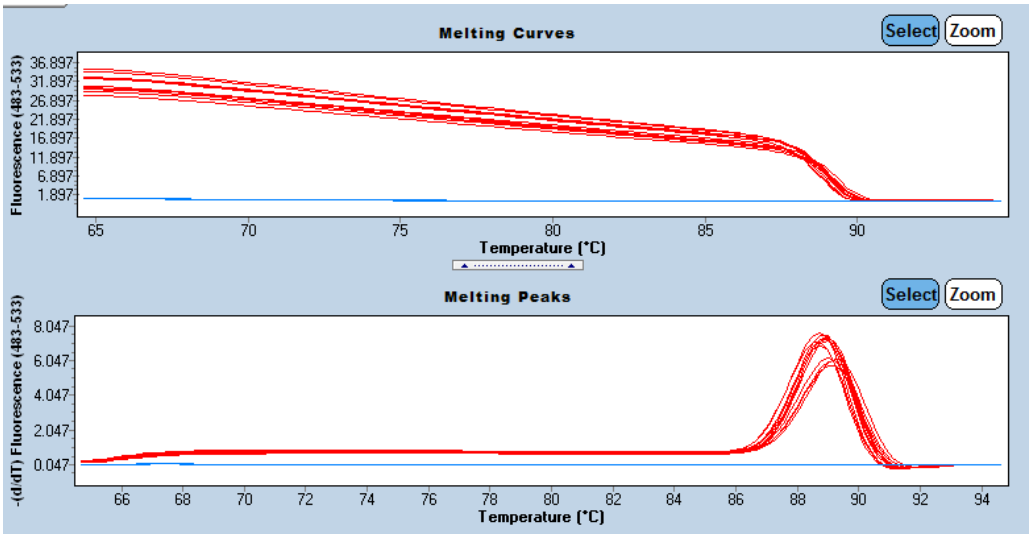


**Mir-ur-3 melting curve**